

Discovery of Prodrug of MRTX1133 as an Oral Therapy for Cancers with KRAS^{G12D} Mutation

Xiang Ji,* Yan Li, Xianqi Kong,* Dawei Chen,* and Jiasheng Lu*

Cite This: *ACS Omega* 2023, 8, 7211–7221

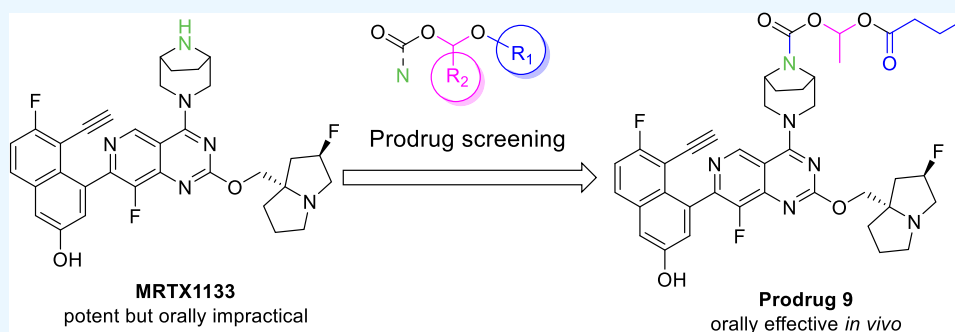
Read Online

ACCESS |

Metrics & More

Article Recommendations

Supporting Information



ABSTRACT: Effective oral therapies are urgently required to treat KRAS^{G12D} mutant cancers. Therefore, synthesis and screening were performed for 38 prodrugs of MRTX1133 to identify an oral prodrug of MRTX1133, a KRAS^{G12D} mutant protein-specific inhibitor. *In vitro* and *in vivo* evaluations revealed prodrug 9 as the first orally available KRAS^{G12D} inhibitor. Prodrug 9 exhibited improved pharmacokinetic properties for the parent compound in mice and was efficacious in a KRAS^{G12D} mutant xenograft mouse tumor model after oral administration.

INTRODUCTION

The guanosine triphosphatase (GTPase) KRAS protein converts guanosine triphosphate (GTP) to guanosine diphosphate (GDP) and is part of the RAS/MAPK signaling pathway important for cell proliferation and differentiation.¹ RAS-mutant cancers account for 20% of human cancers, and >80% of them are related to KRAS isoform mutation, making this mutation a primary target for drug therapy.^{2–4} However, because KRAS protein has a strong binding affinity to GTP and lacks a readily accessible binding pocket for a small molecule, it has been considered an “undruggable target” for decades. Of all, 80% of oncogenic mutations among KRAS mutant tumors occur within codon 12, with the most common mutations being G12D, G12V, and G12C.⁵ The breakthrough in treating KRAS-driven cancers came from a seminal work describing the covalent inhibition of KRAS^{G12C} protein by Shokat and collaborators,⁶ along with the recent clinical development of KRAS^{G12C} inhibitors, such as sotorasib (AMG510) and adagrasib (MRTX849). Both of these compounds occupy an induced switch II pocket in the KRAS^{G12C} protein through irreversible covalent conjugation of cysteine that locks the mutant protein in an inactive (GDP-bound) state, blocking the tumorigenic signaling.^{7–9} However, the KRAS^{G12D} mutation (33% of KRAS mutant tumors) still lacks a proven small-molecule drug for treatment.¹⁰ Recently, Wang et al. identified MRTX1133 as a potent KRAS^{G12D} inhibitor (Figure 1)¹¹ that was efficacious in treating

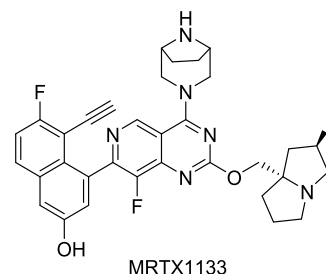


Figure 1. Structure of MRTX1133.

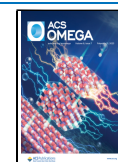
KRAS^{G12D} mutant xenograft mouse tumors via intraperitoneal (IP) administration. However, the inherent physicochemical properties of the compound may hamper further development as an oral therapeutic agent for cancer therapy.¹²

Herein, we exploited the prodrug strategy to improve the oral bioavailability of MRTX1133.

Received: January 16, 2023

Accepted: January 27, 2023

Published: February 9, 2023



RESULTS AND DISCUSSION

The properties of MRTX1133 (Table 1) specify its poor absorption and low oral bioavailability. Particularly,

Table 1. Physicochemical Properties and ADME Profiling Data for MRTX1133

property	value
molecular weight	600.65 ^a
log P	4.61 ^a
hydrogen-bond donor	2 ^a
hydrogen-bond acceptor	11 ^a
rotatable bond count	6 ^a
polar surface area	85.05 ^a
pK _a	7.98 ^a
Caco-2 permeability P _{app}	A – B: 0.48×10^{-6} cm/s B – A: 8.05×10^{-6} cm/s
	efflux ratio: >16.8
t _{1/2} in mouse liver microsomes	38.5 min
CL _{int(liver)}	143 mL/min/kg
absolute bioavailability	0.5% ^b

^aCalculated using ChemOffice software (Chemdraw for Excel). ^b30 mpk oral dose in mouse.

MRTX1133 has a low A – B rate in the Caco-2 permeability assay (Tables 1 and S1). Although not identified as a substrate of P-gp and BCRP transporters, MRTX1133 shows a high B-A rate, namely a high efflux ratio, which is unfavorable for gastrointestinal tract (GI)-absorption. The bioavailability of MRTX1133 is only 0.5% in mice following oral administration at 30 mg per kilogram (mpk). Conversely, MRTX1133 is stable in mouse liver microsomes, and the low oral bioavailability in mice is likely due to poor GI absorption. Thus, many treatment aspects such as increased dosing requirements, high excipient loading, and pill burden will become blockades if MRTX1133 is developed directly as an oral therapeutic.

Hydrogen-bond donors (HBD) are recognized as having antagonistic effects on compound GI absorption.^{13,14} MRTX1133 has two HBD donors: a phenolic group and a secondary amine moiety. The latter is hypothesized to be the major contributor to the poor absorption of the molecule. To test this hypothesis, a series of prodrug compounds were designed and synthesized to mask the amino group HBD for improvement of GI absorption and, ultimately, the oral bioavailability of MRTX1133.

Based on the structural feature and targeting at the secondary amine of MRTX1133, specific promoieties were selected, particularly amide- and carbamate-forming ones that can release parent drugs under the correct conditions.^{15,16} To verify the validity of these identified moieties, several prodrugs of MRTX1133, compounds 1–6 (Figure 2), were synthesized.

An ideal oral prodrug should be stable and absorbed in the GI tract following administration and undergo rapid and complete conversion to the parent compound in compartments such as the liver and blood.¹⁷ Accordingly, compounds 1–6 were first tested *in vitro* for their stability and conversion within simulated gastric fluid (SGF), simulated intestinal fluid (SIF), mouse liver microsomes, and whole blood (Table 2). Compound 1, a carbamate derivative of MRTX1133, was stable during a 30 min incubation in both SGF and SIF and during a 60 min incubation in mouse liver microsomes and in whole blood, without release of the parent compound to a detectable level. These results implied that compound 1 could be stable in the GI tract after oral administration. However, compound 1 may resist conversion to the parent drug even if well absorbed and would enter the circulatory system unchanged because mouse liver microsomes and blood enzymes could not effectively regenerate the parent compound. The carbamate moiety has been used in a prior prodrugs study.¹⁸ However, the intact amyl carbamate of compound 1 under various conditions may result from the electron and steric effects of the secondary aliphatic amine at a bridged position in MRTX1133. A step further from a simple carbamate protection, 1-acyloxy(1-substituted)methyl carbamate protection produced amine prodrugs, including gabapentin enacarbil (for gabapentin) and arbaclofen placarbil (for arbaclofen), which are rapidly converted to the parent drugs by nonspecific esterases.^{19,20} Therefore, this strategy was applied to the secondary amine system in MRTX1133. *In vitro* studies show that compound 2, a 1-(pentanoyloxy)ethyl carbamate of MRTX1133, had high stability in SGF but was moderately labile in SIF. In mouse liver microsomes and whole blood assays, prodrug 2 was efficiently converted to the parent drug. Certain self-immolative promoieties are reported to be particularly useful in prodrugs,^{21–23} and alkyl ester has been used as a trigger for the delivery of drugs.^{24,25} Compound 3 contained an ethyl-ester at the terminal position of the protecting moiety and was readily hydrolyzed in liver microsomes and blood, giving remarkable amounts of de-ethylated intermediate in assay medias (Table S3). However, the subsequent intramolecular cyclization of carboxylate required to extrude the parent drug did not occur as

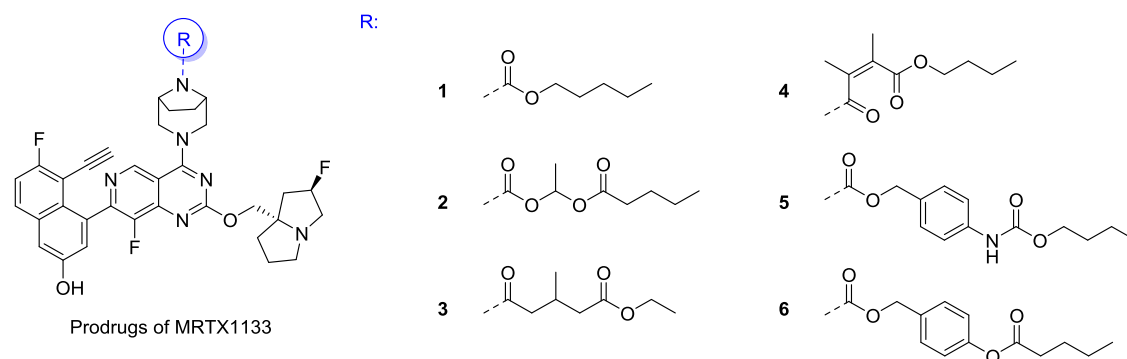


Figure 2. Initial designs for MRTX1133 prodrugs.

Table 2. *In Vitro* Stability of Prodrugs 1–6^a

Cpd	SGF 30 min	SIF 30 min	mouse liver microsomes 60 min ^b		mouse whole blood 60 min	
	prodrug (%)	prodrug (%)	prodrug $t_{1/2}$ (min) ^c	MRTX1133 (%)	prodrug $t_{1/2}$ (min) ^c	MRTX1133 (%)
1	111	115	139	BLQ	stable	BLQ
2	96.2	63.9	0.73	83.0	3.83	111
3	105	110	11.1	BLQ	25.7	BLQ
4	99.5	93.8	35.7	1.4	stable	BLQ
5	98.2	90.4	40.3	16.5	347	0.1
6	106	20	0.61	108	0.65	92.5

^aCpd: compound; BLQ: below the limit of quantification. ^bWith NADPH. ^cHalf-lives shown are based on the disappearance of prodrugs.

expected.²⁴ Similarly, compound 4, protected by a maleate moiety, showed a moderate hydrolytic stability of the ester group in mouse liver microsomes but again failed to release the parent drug under assay conditions; this is inconsistent with examples of a Emetine prodrug, where the point for protection was also a secondary amine in a ring.²⁵ *p*-aminobenzyl carbamate (PABC), a classic self-immolating moiety, was also studied in this earlier work (compound 5). *In vitro* studies show that compound 5 had favorable stability in SGF and SIF and that the butyl carbamate at the terminal decomposed readily in mouse liver microsomes, triggering a subsequent collapse of PABC to generate sufficient amounts of MRTX1133; however, compound 5 had a higher stability in mouse blood, presumably because of the difference in enzyme profiles between blood and liver microsomes. In compound 6, a *p*-hydroxybenzyl group, an *O*-analog of the *p*-aminobenzyl group, replaced that used in compound 5. Compound 6 exhibited a rapid release of MRTX1133 in mouse liver microsomes and in whole blood and had high stability in SGF. However, the stability of SIF was the lowest of the six compounds tested.

Thus, compounds 2 and 6 were expected to have the potential to increase the absorption and oral bioavailability of MRTX1133. Subsequently, the exposure of mice to MRTX1133 released from prodrugs 2 and 6 was assessed following oral administration of the compounds. Remarkable increases in oral bioavailability were observed for both prodrugs (area under the concentration–time curve [AUC] of 380 and 230 ng·h/mL for 2 and 6, respectively) in comparison with that of the parent drug (AUC, 96 ng·h/mL) (Table 3). Although compound 6 exhibited slightly better

Table 3. Oral Bioavailability of MRTX1133 and Prodrugs 2 and 6 in Mice^a

Cpd	administration	dose (mpk)	AUC _{0–24 h} (ng·h/mL)	<i>F</i> (%)	increase in <i>F</i> (fold)
MRTX1133	intravenous	3	2253	N.A.	N.A.
MRTX1133	oral	10	96	1.3	N.A.
2	oral	10 ^b	380	5.1	4.0
6	oral	10 ^b	230	3.1	2.4

^aN.A.: not applicable; Cpd: compound; mpk: mg per kg. ^bNormalized to molar equivalent of the parent compound.

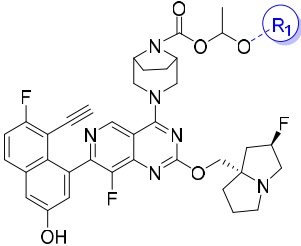
parent drug release than that for compound 2 in both liver microsomes and whole blood assays, the magnitude of the bioavailability (*F*) increase of prodrugs 2 and 6 at an equal-molar dose was 4- and 2.4-fold, respectively. This may be because 2 was more stable in SIF than 6 was, which could be crucial in helping intestinal absorption of the prodrug.

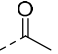
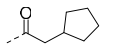
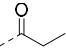
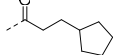
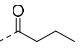
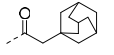
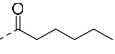
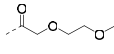
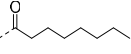
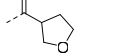
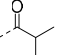
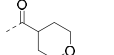
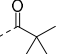
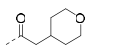
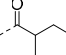
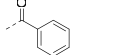
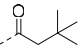
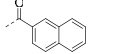
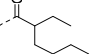
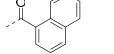
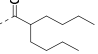
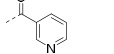
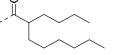
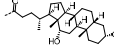
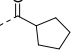
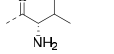
Therefore, the study focused on analogs of compound 2, i.e., 1-(acyloxy)ethyl carbamate.

A series of prodrugs (7–32) were synthesized and evaluated in mice for their oral bioavailability. Based on the feature of the R₁-group in the moiety, the 26 compounds were categorized into six subgroups: straight-chain acyl (7–11), branched-chain acyl (12–18), carbocyclic-containing acyl (19–22), etherate-containing acyl (23–26), aromatic acyl (27–30), and other (31 and 32). Structure details and absorption data are depicted in Table 4.

Most of the prodrugs increased the bioavailability of the parent drug by more than 2-fold, except for compounds 22, 23, and 32. In the straight-chain acyl sub-group of prodrugs, the carbon number in R₁ covers 1–7. Compound 9 was most effective with three carbons in R₁ and had a 6.2-fold increase in bioavailability (7.9%) compared with that following direct administration of the parent drug. R₁ carbon number increase (compounds 2, 10, and 11) or decrease (compounds 7 and 8) lowered the oral bioavailability for the parent drug. Similarly, all the prodrugs in the branched-chain acyl subgroups exhibited a 2.4- (18) to 6.2-fold (12 and 14) increase in bioavailability for the parent drug. A small, three-carbon isopropyl as R₁ (compound 12) was again most effective among all the compounds in this sub-group; an increase in the number of carbon atoms in R₁ either decreased the bioavailability of the drug in most of the cases or did not increase the bioavailability (as for compound 14). In addition to the straight- and branched-chain aliphatic R₁, the cyclic-aliphatic R₁ was introduced into prodrugs 19–22. Among these four, compound 20, with a moderately sized R₁, produced the highest bioavailability (*F*, 7.1%) of the parent drug, whereas compound 22, having a bulky R₁, only produced 1.6% bioavailability, the lowest among all the prodrugs evaluated in this study. The increase in the size of the aliphatic R₁ would be expected to increase lipophilicity (as *c* log *P*) and hydrolytic stability (Table S2), which could be helpful in absorption and increase bioavailability. This does not appear to be the case with this series of prodrugs.

The alkyl group remarkably increases the lipophilicity of a compound with an increasing number of carbons, whereas replacing carbon with a heteroatom such as oxygen could balance the lipophilicity and hydrophilicity. Favorable oral absorption is known to coincide with appropriate amphipathic properties of the molecule.²⁶ Therefore, prodrugs 23–26 were synthesized with the aim that the oxygen atoms in R₁ would balance the prodrug properties and benefit absorption. However, the desired result was not obtained by this variation. For example, replacing the one ring-carbon in 19 with an oxygen resulted in compound 24, which decreased the bioavailability of the parent drug, from 5.6 to 3.3%. The optimum compound in this sub-group, 26, provided a

Table 4. Bioavailability^a for MRTX1133 from Prodrugs 7–32 in Mice


Cpd	R1	AUC _{0–24h} (ng·h/mL)	F (%)	Cpd	R1	AUC _{0–24h} (ng·h/mL)	F (%)
7		557	7.4	20		538	7.2
8		282	3.8	21		334	4.5
9		595	7.9	22		120	1.6
10		295	3.9	23		164	2.2
11		345	4.6	24		250	3.3
12		591	7.9	25		323	4.3
13		359	4.8	26		513	6.8
14		590	7.9	27		546	7.2
15		355	4.7	28		291	3.9
16		252	3.4	29		261	3.5
17		252	3.4	30		204	2.7
18		232	3.1	31		279	3.7
19		424	5.7	32		186	2.5

^aAll compounds (Cpd) were dosed at molar equivalent to 10 mpk of MRTX1133.

relatively favorable bioavailability of MRTX1133 at 6.8% (*F*), which was no better than that of the closest carbon analog (**20**; *F*, 7.2%). The same trend was observed when comparing the results from compounds **23** and **10**.

Studies were extended to aromatic R₁, including compounds **27–30**. In this sub-group of prodrugs, compound **27**, where R₁ was the simplest phenyl, provided an acceptable oral

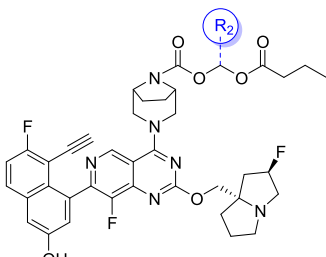
bioavailability of 7.2%. Changing the phenyl to naphthyl or pyridyl remarkably lowered the drug's bioavailability.

Prodrug **31** was designed to exploit an intestinal bile acid transporter with a deoxy cholyl group as $R_1-C(O)-$. It exhibited higher bioavailability than MRTX1133, albeit not to a considerable level. Similarly, amino acids are used in many prodrugs to enhance absorption using specific transporters in intestinal epithelial cells.²⁷ However, prodrug **32**, with *L*-valyl as $R_1-C(O)-$, only exhibited a bioavailability of 2.5% (<2-fold increase).

Thus, five of 28 prodrugs (compounds **9**, **12**, **14**, **20**, and **27**; Tables 3 and 4) evaluated in mice exhibited a bioavailability of >7%. The most effective R_1 compounds are from aliphatic-chain subgroups with three (**9** and **12**) or four (**14**) carbons.

Further structural variation of the promoity was assessed using R_2 (see the structure presented in Table 5). As discussed

Table 5. Bioavailability^a of MRTX1133 from Prodrugs 33–38 in Mice



Cpd	R2	AUC _{0–24h} (ng·h/mL)	F(%)
33	H	349	4.7
34	CH ₂ CH ₂ CH ₃	594	7.9
35	CH ₂ CH ₂ CH ₂ CH ₃	89.5	1.2
36	CH(CH ₃) ₂	295	3.9
37	Cyclobutyl	470	6.3
38	Cyclohexyl	436	5.8

^aAll compounds (Cpd) were dosed at a molar equivalent of 10 mpk of MRTX1133.

above, compounds **9**, **12**, and **14** had the same or highly similar bioavailabilities compared with that of the parent drug; the corresponding acids for these three compounds are butyric, isobutyric, and isovaleric acid, respectively. Butyric acid is a common short-chain fatty acid used in medicinal chemistry that has no *in vivo* safety concerns.²⁸ In addition, butyryl is the simplest group among the three. Therefore, compound **9** was

selected as the starting point for searching the optimal R_2 group for the study and compounds **33–38** were synthesized for pharmacokinetic evaluation in mice. Pharmacokinetic (PK) results are summarized in Table 5.

R_2 modification failed to improve the bioavailability of the parent drug either through increasing or reducing the size of R_2 (Table 5). Compound **34** produced the most bioavailability, although this only matched that of compound **9**. This observation may indicate that the R_2 group cannot be bigger or bulkier because of steric effects. R_2 should contain at least one carbon atom; otherwise, the methylene acetal (**33**: R_2 , H) may be too labile to maintain favorable bioavailability (Table S2).

In summary, compound **9** was the most effective of the prodrugs evaluated in this study and was therefore selected for additional investigation based on the 6.2-fold increase in bioavailability of MRTX1133 and the low safety concerns of the components of the promoity.^{28,29} Evaluation of compound **9** stability in microsomes, whole blood, and intestinal S9 fraction was performed using different animal species. The results (Tables S4 and S5) imply that compound **9** has comparable stability profiles across animal species and may have even better outcomes in higher animals, supporting the evaluation of compound **9** in *in vivo* studies.

To understand the dose response in bioavailability, two doses (10 and 30 mpk) of compound **9** and MRTX1133 were evaluated in mice, together with a much higher dose (100 mpk) of compound **9**. The PK data from this study are given in Table 6, and the blood concentration–time curves are

Table 6. Bioavailability of MRTX1133 from MRTX1133 and Prodrug **9 in Mice**

Cpd	dose (mpk)	AUC _{0–24h} (ng·h/mL)	F (%)
MRTX1133	10	96	1.3
MRTX1133	30	102	0.5
9	10 ^a	595	7.9
9	30 ^a	1501	6.7
9	100 ^a	4414	5.9

^aDose for compound **9** is normalized (corrected to mole-equivalent dose of parent drug).

presented in Figure 3. MRTX1133 did not show a dose response, and the AUC value for the drug was 102 ng·h/mL at 30 mpk compared with 96 ng·h/mL at 10 mpk, indicating a low ceiling for the system exposure. If the *F* values are compared between the two doses, the bioavailability drops dramatically (1.3–0.5%) with increasing dose (10–30 mpk, respectively). A clear dose response for prodrug **9** was shown in the AUC value from the dose of 10–30 mpk (1501 and 4414 ng·h/mL, respectively), although this was not perfectly proportional. This property is important for dose escalation at the development stage. The bioavailability parameter, *F* (%) decreased slightly with dose increase; however, the bioavailability for the parent drug remained at 5.9% at a dose of 100 mpk (the highest dose tested). Further increases in dose to 300 mpk became intolerable to mice, likely because of the C_{max} -driven toxicity of the parent drug. Therefore, prodrug **9** was potentially a favorable compound for further development.

An important aspect for a drug with toxicity liability is to have a low C_{max} but an extended period of “effective concentration” in the system. The MRTX113 blood concentrations at various time points are given in Table 7.

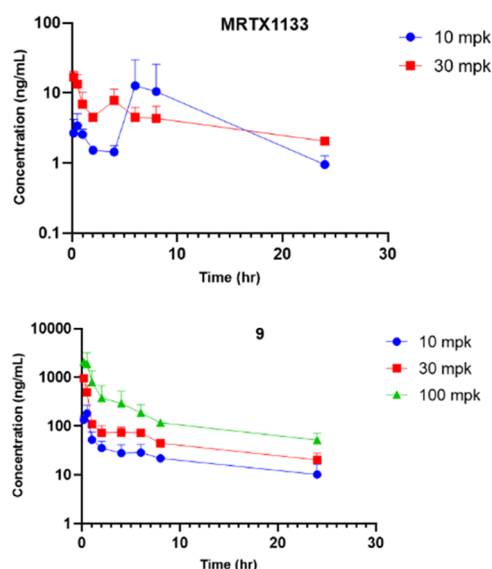


Figure 3. Blood concentration–time curve of MRTX1133 in mice. Top panel, after oral administration of MRTX1133; bottom panel, after oral administration of prodrug 9 (dose normalized to molar equivalent of parent drug).

Table 7. Changes in MRTX1133 Blood Concentration with Time after Oral Administration of Mice with Different Doses of Prodrug 9

time (h)	MRTX1133 concentration (ng/mL)		
	10 mpk ^a	30 mpk ^a	100 mpk ^a
0.167	134.8	961.0	2083.3
0.5	182.6	497.0	1891.0
1	52.5	109.6	800.2
2	35.7	73.5	380.5
4	27.9	74.4	293.0
6	28.7	73.1	189.0
8	21.9	44.9	118.1
24	10.2	20.3	52.0

^aDose for compound 9 is normalized (corrected to mole-equivalent dose of parent drug). mpk: mg per kg.

At a 100 mpk oral dose of prodrug 9, the blood concentration of MRTX113 is maintained >100 ng/mL for >8 h, which is a meaningful level for suppression of KRAS signaling.¹¹ This result indicates that prodrug 9 could be administered twice a day to maintain the blood concentration of MRTX1133 for evaluation of efficacy in mice. Accordingly, a xenograft tumor mouse model (pancreatic cancer cell line AsPC-1, bearing the KRAS^{G12D} mutation) was constructed for evaluating the antitumor efficacy of prodrug 9 as an oral therapeutic agent.

Treatment was started at a tumor size of 200 mm³. Animals were treated with a low and high dose (37.8 and 126 mpk, respectively) of prodrug 9, corresponding to equimolar doses of MRTX113 at 30 and 100 mpk, respectively. Two control groups were treated in the same schedule either with MRTX1133 at 100 mpk or with a dosing vehicle for comparison. All treatments were administered via oral gavage twice a day and continued for 16 days. At the end of the study, the group treated with 9 at a high dose showed a tumor growth inhibition (TGI) of 54%, while the group treated with a low dose showed a 20% TGI.

In contrast, the MRTX1133-treated group showed no apparent antitumor effect. The detailed measurements of tumor size for each group are presented in Figure 4. Compared

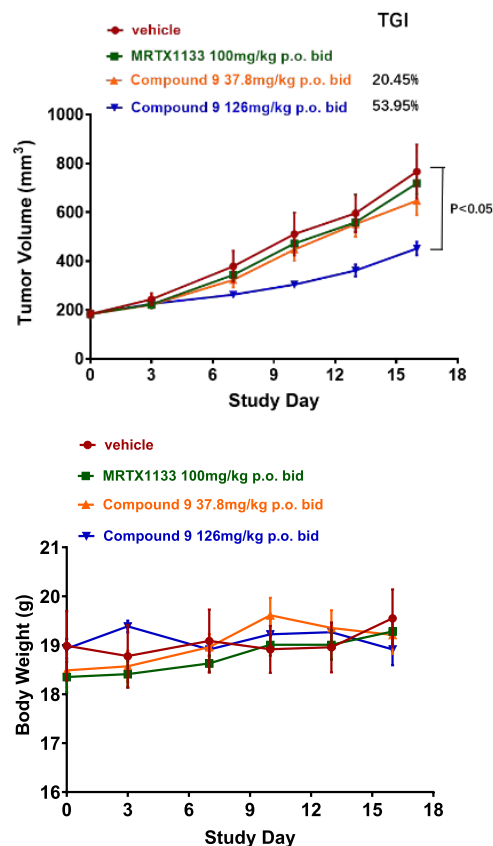


Figure 4. Efficacy of prodrug 9 in AsPC-1 model. Differences in mean tumor volume between vehicle and treated cohorts were assessed using a two-tailed Student's *t* test with equal variance.

with the vehicle group or the MRTX1133 group, no apparent change in body weight was observed in the groups treated with both doses of compound 9 throughout the treatment, indicating the safety of prodrug 9.

To gain insight into the behavior of prodrug 9 *in vivo* and the impact on the pharmacodynamics of the parent drug, blood and tumor concentrations of prodrug 9 and MRTX1133 were analyzed at 2 and 8 h following the last dose in the efficacy study (high dose). The concentration of prodrug 9 in blood was below detection level even at 2 h post oral dosing, which was consistent with the short half-life in mouse blood (Table S2). However, the prodrug was present in tumor tissue at 116 and 317 ng/g at 2 and 8 h, respectively (Table 8), implying prodrug accumulation in the tumor. These results provide direct evidence for the stability of prodrug 9 in the GI tract of

Table 8. Blood and Tumor Concentration of Drug and Prodrug^a

Cpd	blood (ng/mL)		tumor (ng/g)	
	2 h ^b	8 h ^b	2 h ^b	8 h ^b
9	BLQ	BLQ	116	317
MRTX1133	234	114	2113	2440

^aCpd: compound. BLQ: below the limit of quantification. ^bTime post last oral dose in the tumor model.

mice and its tolerability to first-pass metabolism, regardless of the short half-life in mouse liver microsomes and intestinal homogenates as indicated by the *in vitro* assays (Tables S4 and S5). Prodrug 9 was absorbed following oral administration and can penetrate tumors. The results suggest that the conversion of prodrug 9 to the parent drug differs between that in a tumor and that in blood. The concentration of MRTX1133 (the parent drug) was 9-fold higher in tumor tissues than in blood at 2 h and 21-fold higher at 8 h, following the last dose of the prodrug, implying that oral administration of the prodrug 9 provided a sustainable therapeutic effect (Table 8).

Comparing the tissue distribution of MRTX1133 following administration of the prodrug and parent drug could increase understanding of the prodrug's properties. However, difficulties arose because the oral bioavailability of MRTX1133 was too low to enable such a comparison. Thus, studies were conducted to compare oral administration of prodrug 9 (dose: molar equivalent to 100 mpk MRTX1133) with IP of MRTX1133 (dose: 10 mpk MRTX1133) in mice.

Following IP administration of MRTX1133, the highest drug concentration was found in the kidney, at ~285 000 and 334 000 ng/g at 2 and 8 h, respectively (Table 9), followed by

Table 9. Tissue Distribution of MRTX1133

tissue	concentration ^b of MRTX1133			
	from MRTX1133(IP)		from prodrug 9 (oral)	
	2 h ^a	8 h ^a	2 h ^a	8 h ^a
blood	654	330	234	144
tumor	11 870	14 300	2113	2440
heart	18 330	15 795	4307	5240
liver	63 525	62 950	8190	9380
spleen	58 450	54 025	5177	6797
lung	53 040	57 300	19 680	19 500
kidney	285 150	333 900	33 380	45 660
stomach	26 325	27 775	33 800	16 583
intestine	24 388	18 213	72 817	63 833
brain	131	139	80.7	70.4

^aTime post last oral dose in the tumor model. ^bUnit for blood is ng/mL and for other organs it is ng/g.

that in the liver, spleen, and lung (at ~60 000 ng/g), which was ~5-fold lower than that in the kidney. The concentration in the stomach, intestine, and heart was even lower (~20 000 ng/g). Interestingly, after oral administration of prodrug 9, the highest concentration of MRTX1133 was found in the intestine at both time points, followed by that in the kidney, lung, and stomach. In contrast, oral administration of prodrug 9 produced a relatively even distribution of MRTX1133 among most of the major organs (Figures S1 and S2). Notably, drug accumulation was remarkably shifted to the intestine, lung, and stomach with the oral administration of prodrug 9. Furthermore, a high concentration of prodrug 9 was detected in the stomach post oral dosing, which has no clear explanation and merits further study (Figure S2). Nevertheless, these results demonstrated that the tissue distribution of MRTX1133 was substantially altered using prodrug administration, which provides a more beneficial safety profile and potential advantages in treating KRAS^{G12D}-driven cancers in specific organs.

Lipid-based drug delivery systems such as self-microemulsifying drug delivery systems (SMEEDS) and self-nanoemulsifying drug delivery systems (SNEEDS) have

attracted attention in pharmaceutical science in improving the oral bioavailability of drugs.^{30,31} Prodrug 9 possessed a high *c log P* (8.11) and is a good candidate for evaluating the enhancement of prodrug absorption and parent drug bioavailability by lipid-based formulation. Consequently, several off-the-shelf lipid-based formulations were prepared as dosing vehicles for prodrug 9 for PK studies in mice (Table S6). When prodrug 9 was administered with a particular lipid-based formulation (Table 10), the systemic exposure

Table 10. PK Parameters for MRTX1133 Following Oral Administration of Prodrug 9 (37.8 mpk) with Different Lipid-Based Formulations

formulation	AUC _{0–24 h} (ng·h/mL)	F (%)	C _{max} (ng/mL)	T _{max} (h)
conventional ^a	1501	6.7	961	0.17
lipid based ^b	2667	11.8	229	1.83

^aDimethyl sulfoxide/Solutol/(20%SBE- β -CD) = 5:5:90 (v/v/v).

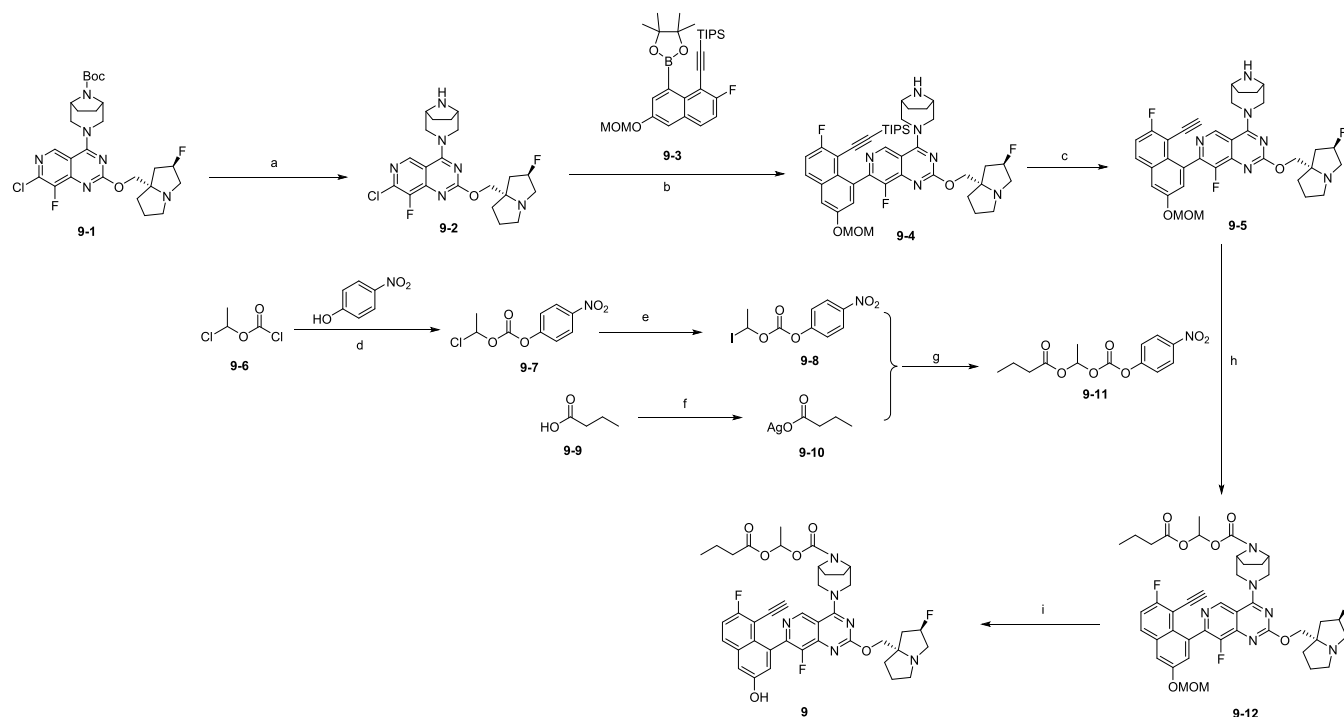
^bLabrafac WL 1349/Kolliphor EL/Transcutol HP = 15:40:45 (w/w/w).

(AUC_{0–24 h}) of MRTX1133 in mice was almost doubled, and the oral bioavailability (*F*, %) for MRTX1133 increased to 11.8%. Moreover, the PK parameters featured a suppressed C_{max} and delayed T_{max} of parent drug MRTX1133, which would be expected to lead to (1) the amelioration of C_{max}-related toxicity in animals observed at high dosage (see above) and (2) the prolongation of the effective concentration of MRTX1133 in the system. Use of lipid-based formulation with a 300 mpk oral dose was well-tolerated in mice despite this dose level being impossible otherwise because of toxicity. More importantly, the optimized PK profiles showed a sustained effective concentration of MRTX1133 in blood over time (Table S7). Therefore, a lipid-based formulation is in further development that will enable prodrug 9 to achieve improved antitumor efficacy with a higher dosage and even longer dosing interval.

The synthesis of prodrug 9 (Scheme 1) commenced with the deprotection of 9-1 with a solution of HCl in dioxane, which was subsequently coupled with 9-3 to afford 9-4, followed by deprotection with tetrabutylammonium fluoride (TBAF) to produce 9-5. Another intermediate 9-11 was synthesized as previously described and then reacted with 9-5 under a basic condition to afford 9-11. The deprotection of 9-12 was conducted readily in HCl dioxane solution to produce prodrug 9.^{32–34}

CONCLUSIONS

A systemic, step-by-step strategy was applied to design and synthesize a series of carbamate-based prodrugs of MRTX1133. A combined PK study and efficacy evaluation in an animal model identified prodrug 9 as an orally bioavailable compound for KRAS^{G12D} mutant inhibitor MRTX1133. Prodrug 9 features a 1-(butyryloxy)ethyl carbamate promoeity that masks the secondary amine group in the parent compound, which suppresses the negative effect on the permeability and absorption of the amine group and considerably improves the systemic exposure and oral bioavailability of MRTX1133 in mice. In the murine animal model, prodrug 9 exhibited an antitumor activity with the advantages of no weight loss and no considerable signs of toxicity. A study of drug (and prodrug) distribution in tissues revealed that oral administration of prodrug 9 not only enabled

Scheme 1. Synthesis of Prodrug **9**^a

^aReagents and conditions. (a) HCl in dioxane, MeOH, room temperature (rt), 2 h, 100%; (b) Pd(dppf)Cl₂·CH₂Cl₂, Cs₂CO₃, dioxane/water, 100 °C, 2 h, 75.06%; (c) TBAF, THF, 1 h, 59.02%; (d) Et₃N, DCM, room temperature, 1 h, 50.93%; (e) NaI, acetone, 50 °C, 30 h, 60.48%; (f) Ag₂O, acetonitrile/water, room temperature, 16 h, 24.85%; (g) toluene, 50 °C, overnight, 47.51%; (h) Et₃N, DMAP, DCM, 40 °C, 1 h, 65.93%; (i) HCl in dioxane, MeOH/DCM, 15 min, 80.07%.

MRTX1133 accumulation in tumor tissue but also results in an optimal distribution of MRTX1133 in organs highly related to KRAS^{G12D}-driven tumors. In addition, the PK profiles of MRTX1133, following administration of prodrug **9**, were favorably modified using increasing prodrug formulated in lipid-based dosing media, indicating the possibility for increased oral bioavailability and safety in future research and development. To the best of our knowledge, this is the first report of an oral small-molecule KRAS^{G12D} inhibitor, and our data support prodrug **9** as an oral drug candidate for future drug development.

EXPERIMENTAL SECTION

All chemicals were purchased from commercial suppliers and used as received, unless otherwise indicated. Proton nuclear magnetic resonance (¹H NMR) spectra and carbon nuclear magnetic resonance (¹³C NMR) spectra were recorded on Zhongke-Niujin AS500 500 MHz spectrometers. Data are reported as follows: chemical shift, multiplicity (s = singlet, d = doublet, t = triplet, q = quartet, h = sextet, bs = broad singlet, dd = doublet of doublet, dt = doublet of triplet, and m = multiplet), coupling constants, and number of protons. Unless otherwise noted, all reported compounds are ≥95% pure as determined by high-performance liquid chromatography (HPLC). HPLC conditions were: XBridge C18 4.6 mm × 100 mm, 3.5 μm, 5–95% acetonitrile in water (0.1% diethylamine; DEA), 14.0 min run, flow rate 1 mL/min, ultraviolet (UV) detection (λ = 220, 254 nm). Mass spectra were obtained using liquid chromatography-mass spectrometry (LCMS) on a Waters e2695 using electrospray ionization (ESI; positive mode). LCMS conditions were: XBridge C18 4.6 mm × 100 mm, 3.5 μm, 5–95% CAN in water (0.1%

DEA), 14.0 min run, flow rate 1 mL/min, UV detection (λ = 220, 254 nm). All experiments utilizing animals were conducted under protocols approved by the Qpex Institutional Animal Care and Use Committee.

Preparation of Compound 9. 4-((1*R*,5*S*)-3,8-Diazabicyclo[3.2.1]octan-3-yl)-7-chloro-8-fluoro-2-(((2*R*,7*aS*)-2-fluorotetrahydro-1*H*-pyrrolizin-7*a*(5*H*)-yl)-methoxy)pyrido[4,3-*d*]pyrimidine (**9-2**). HCl (4 M) in dioxane (50 mL) was added to a solution of compound **9-1** (7 g, 12.7 mmol, 1.0 equiv) in methanol (MeOH) (30 mL). The mixture was stirred at room temperature for 2 h, then concentrated *in vacuo*. The pH of the residue was adjusted to 8 with aqueous NaHCO₃. The mixture was diluted with MeOH and concentrated *in vacuo*. The residue was dissolved with dichloromethane (DCM) and filtered. The filtrate was concentrated *in vacuo* to afford crude compound **9-2** (6.0 g, 100% yield).

4-((1*R*,5*S*)-3,8-Diazabicyclo[3.2.1]octan-3-yl)-8-fluoro-7-(7-fluoro-3-(methoxymethoxy)-8-((triisopropylsilyl)ethynyl)-naphthalen-1-yl)-2-(((2*R*,7*aS*)-2-fluorotetrahydro-1*H*-pyrrolizin-7*a*(5*H*)-yl)methoxy)pyrido[4,3-*d*]pyrimidine (**9-4**).³² Compound **9-2** was added to a solution of compound **9-3** (4.09 g, 7.98 mmol, 1.2 equiv) in dioxane (50 mL), followed by addition of Cs₂CO₃ (6.5 g, 19.96 mmol, 3 equiv) in water (20 mL), Pd(dppf)Cl₂·CH₂Cl₂ (810 mg, 1 mmol, 0.15 equiv). The mixture was stirred at 100 °C for 2 h under nitrogen atmosphere, then cooled to room temperature. The mixture was diluted with water and DCM. The organic phase was washed with water and brine, dried over Na₂SO₄, filtered, and concentrated. The residue was purified using flash column chromatography (MeOH/DCM with 0.1% triethylamine

[TEA] = 0–5%) to afford compound **9-4** (4 g, 75.1% yield). LCMS [ESI, M⁺]: 801.7.

4-((1*R*,5*S*)-3,8-Diazabicyclo[3.2.1]octan-3-yl)-7-(8-ethynyl-7-fluoro-3-(methoxymethoxy)naphthalen-1-yl)-8-fluoro-2-(((2*R*,7*aS*)-2-fluorotetrahydro-1*H*-pyrrolizin-7*a*(5*H*)-yl)-methoxy)pyrido[4,3-*d*]pyrimidine (**9-5**). A 1 M tetrabutylammonium fluoride (TBAF) in tetrahydrofuran (THF) (25 mL, 25 mmol, 5 equiv) was added to a solution of compound **9-4** (4 g, 5 mmol, 1 equiv) in THF (40 mL). The reaction mixture was stirred at room temperature for 1 h and concentrated *in vacuo*. The residue was purified using flash column chromatography (MeOH/DCM with 0.1% TEA = 0–6%) to afford compound **9-5** (1.9 g, 59.0% yield). ¹H NMR: (500 MHz, CD₃OD) δ 9.02 (s, 1H), 7.98 (dd, *J* = 9.0, 5.6 Hz, 1H), 7.68 (s, 1H), 7.43–7.34 (m, 2H), 5.36 (s, 2.5H), 5.25 (s, 0.5H), 4.61 (dd, *J* = 20.8, 11.1 Hz, 2H), 4.26 (dt, *J* = 16.7, 10.4 Hz, 2H), 3.77–3.61 (m, 4H), 3.51 (s, 3H), 3.39 (d, *J* = 8.9 Hz, 1H), 3.29–3.14 (m, 3H), 3.01 (dd, *J* = 14.2, 9.0 Hz, 1H), 2.39–2.11 (m, 3H), and 2.04–1.73 (m, 7H). LCMS [ESI, M⁺]: 645.5.

1-Chloroethyl (4-Nitrophenyl) Carbonate (**9-7**). Et₃N (16.99 g, 167.87 mmol, 1.2 equiv) was added to a solution of *p*-nitrophenol (21.41 g, 153.88 mmol, 1.1 equiv) in DCM (96.23 mL). Compound **9-6** (20 g, 139.89 mmol, 1 equiv) was added to the mixture at 0 °C. The mixture was warmed to room temperature, stirred at this temperature for 1 h, and then diluted with water. The organic phase was washed with brine, dried over Na₂SO₄, filtered, and concentrated. The residue was purified using flash column chromatography (petroleum ether [PE]/ethyl acetate [EA] = 0–6%) to afford compound **9-7** (17.5 g, 50.9% yield). ¹H NMR: (500 MHz, CDCl₃) δ ppm δ 8.30 (d, *J* = 8.8 Hz, 2H), 7.42 (d, *J* = 8.8 Hz, 2H), 6.50 (q, *J* = 5.7 Hz, 1H), and 1.93 (d, *J* = 5.7 Hz, 3H).

1-Iodoethyl (4-Nitrophenyl) Carbonate (**9-8**).³³ NaI (24.41 g, 162.86 mmol, 4 equiv) was added to a solution of compound **9-7** (10 g, 40.71 mmol, 1 equiv) in acetone (100 mL). The mixture was stirred at 50 °C for 30 h under nitrogen atmosphere, then cooled to room temperature and filtered. The filtrate was concentrated, and the residue was purified using flash column chromatography (PE/EA = 0–3%) to afford compound **9-8** (8.3 g, 60.5% yield).

Silver Butyrate (**9-10**). Ag₂O (31.56 g, 136 mmol, and 0.6 equiv) was added to a solution of *n*-butyric acid **9-9** (20 g, 227 mmol, and 1 equiv) in acetonitrile (200 mL) and water (100 mL). The mixture was stirred at room temperature for 16 h and filtered. The filtrate was concentrated *in vacuo* to afford silver butyrate **9-10** (11 g, 24.9% yield).

1-(((4-Nitrophenoxy)carbonyloxy)ethyl butyrate (**9-11**).³³ Silver butyrate **9-10** (2.53 g, 12.96 mmol, 1.15 equiv) was added to a solution of compound **9-8** (3.8 g, 11.27 mmol, 1 equiv) in toluene (38 mL). The mixture was heated to 50 °C and stirred at this temperature overnight, then cooled to 25 °C and filtered. The filtrate was concentrated, and the residue was purified using flash column chromatography (PE/EA = 0–3%) to afford compound **9-11** (1.59 g, 47.5% yield). ¹H NMR: (500 MHz, CD₃OD) δ 8.32 (d, *J* = 9.1 Hz, 2H), 7.48 (d, *J* = 9.1 Hz, 2H), 6.83 (q, *J* = 5.4 Hz, 1H), 2.37 (t, *J* = 7.3 Hz, 2H), 1.66 (h, *J* = 7.4 Hz, 2H), 1.58 (d, *J* = 5.4 Hz, 3H), and 0.97 (t, *J* = 7.4 Hz, 3H).

1-(Butyryloxy)ethyl (1*R*,5*S*)-3-(7-(8-ethynyl-7-fluoro-3-(methoxymethoxy)naphthalen-1-yl)-8-fluoro-2-(((2*R*,7*aS*)-2-fluorotetrahydro-1*H*-pyrrolizin-7*a*(5*H*)-yl)methoxy)pyrido[4,3-*d*]pyrimidin-4-yl)-3,8-diazabicyclo[3.2.1]octane-8-car-

boxylate (**9-12**). Compound **9-11** (1.58 g, 5.3 mmol, 1.8 equiv) was added to a solution of compound **9-5** (1.9 g, 2.95 mmol, 1 equiv) in DCM (19 mL), followed by the addition of Et₃N (745.56 mg, 7.37 mmol, 2.5 equiv) and dimethylamino-pyridine (DMAP) (72.01 mg, 0.589 mmol, 0.2 equiv). The mixture was stirred at 40 °C for 1 h, then concentrated. The residue was purified by flash column chromatography (MeOH/DCM = 0–3%) to afford compound **9-12** (1.56 g, 65.9% yield). ¹H NMR: (500 MHz, CD₃OD) δ 9.03 (s, 1H), 7.98 (dd, *J* = 9.0, 5.7 Hz, 1H), 7.68 (d, *J* = 2.4 Hz, 1H), 7.45–7.34 (m, 2H), 6.86 (q, *J* = 5.2 Hz, 1H), 5.36 (s, 2.5H), 5.25 (s, 0.5H), 4.67 (bs, 2H), 4.48 (bs, 2H), 4.28 (dt, *J* = 17.1, 10.4 Hz, 2H), 3.78 (s, 2H), 3.51 (s, 3H), 3.41 (d, *J* = 7.9 Hz, 1H), 3.30–3.13 (m, 3H), 3.02 (dt, *J* = 9.5, 5.5 Hz, 1H), 2.42–2.09 (m, 5H), 2.07–1.79 (m, 7H), 1.65 (s, 2H), 1.53 (s, 3H), 0.97 (t, *J* = 7.1 Hz, 3H). LCMS [ESI, M⁺]: 803.6.

1-(Butyryloxy)ethyl (1*R*,5*S*)-3-(7-(8-ethynyl-7-fluoro-3-hydroxynaphthalen-1-yl)-8-fluoro-2-(((2*R*,7*aS*)-2-fluorotetrahydro-1*H*-pyrrolizin-7*a*(5*H*)-yl)methoxy)pyrido[4,3-*d*]pyrimidin-4-yl)-3,8-diazabicyclo[3.2.1]octane-8-carboxylate (**9**). MeOH (0.5 mL) was added to a solution of compound **9-12** (1.56 g, 1.94 mmol, 1.0 equiv) in DCM (100 mL), followed by the addition of another solution of 4 M HCl in dioxane (6 mL). The reaction mixture was stirred at room temperature for 15 min and concentrated *in vacuo*. The residue was diluted with DCM, the pH was adjusted with Et₃N, and it was then concentrated again. The residue was diluted with DCM, washed with water and brine, dried over Na₂SO₄, filtered, and concentrated. The residue was purified using flash column chromatography (MeOH/DCM = 0–5%) to afford compound **9** (1.2 g, 80.1% yield). ¹H NMR: (500 MHz, CD₃OD) δ 9.05 (s, 1H), 7.89 (dd, *J* = 8.9, 5.9 Hz, 1H), 7.40–7.30 (m, 2H), 7.24 (s, 1H), 6.89 (q, *J* = 5.1 Hz, 1H), 5.34 (d, *J* = 54.5 Hz, 1H), 4.71 (bs, 2H), 4.51 (bs, 2H), 4.31 (dt, *J* = 16.9, 10.5 Hz, 2H), 3.82 (s, 2H), 3.39 (d, *J* = 7.8 Hz, 1H), 3.33–3.18 (m, 3H), 3.05 (dt, *J* = 9.4, 5.2 Hz, 1H), 2.46–2.14 (m, 5H), 2.07–1.86 (m, 7H), 1.69 (s, 2H), 1.57 (s, 3H), 1.00 (t, *J* = 7.3 Hz, 3H); ¹³C NMR: (126 MHz, CD₃OD): δ 173.65, 173.38, 167.05, 165.58, 165.20, 163.22, 155.59, 153.56, 153.19, 151.51, 150.31, 150.22, 146.95, 146.83, 145.05, 134.57, 134.23, 131.56, 131.49, 127.11, 124.13, 117.16, 116.95, 113.09, 112.41, 105.52, 105.38, 99.46, 98.06, 91.17, 90.04, 76.19, 75.76, 74.60, 61.39, 61.24, 58.32, 55.83, 55.37, 43.53, 43.37, 37.15, 36.79, 27.94, 27.23, 26.30, 20.01, 19.25, 13.85; LCMS [ESI, M⁺]: 759.3.

■ ASSOCIATED CONTENT

Supporting Information

The Supporting Information is available free of charge at <https://pubs.acs.org/doi/10.1021/acsomega.3c00329>.

Synthetic experimental procedures for compounds **1–38**; NMR spectra and HPLC trace of final compounds; *in vitro* stability studies; *in vivo* PK and TGI studies; results of tissue distribution and Caco-2 permeability (PDF)

■ AUTHOR INFORMATION

Corresponding Authors

Xiang Ji – Department of Biochemistry, School of Life Sciences, Fudan University, Shanghai 200437, China; Risen (Shanghai) Pharma Tech Co., Ltd., Shanghai 201210, China; orcid.org/0000-0002-8434-2328; Email: xiang.ji@risen-group.com

Xianqi Kong – Risen (Shanghai) Pharma Tech Co., Ltd., Shanghai 201210, China; Email: xianqi.kong@risen-group.com

Dawei Chen – Risen (Shanghai) Pharma Tech Co., Ltd., Shanghai 201210, China; Email: dawei.chen@risen-group.com

Jiasheng Lu – Risen (Shanghai) Pharma Tech Co., Ltd., Shanghai 201210, China; Guangdong Key Laboratory of Nanomedicine, Chinese Academy of Sciences, Shenzhen 518055, China; Email: jiasheng.lu@risen-group.com

Author

Yan Li – Risen (Shanghai) Pharma Tech Co., Ltd., Shanghai 201210, China

Complete contact information is available at:

<https://pubs.acs.org/10.1021/acsomega.3c00329>

Author Contributions

The manuscript was written through contributions of all authors. All authors have given approval for the final version of the manuscript.

Notes

The authors declare no competing financial interest.

ACKNOWLEDGMENTS

This work was sponsored by Risen (Shanghai) Pharma Tech Co., Ltd. The authors would like to thank the following teams/people for their valuable contributions to this work. Chemistry team (Risen Pharma Tech Co., Ltd., Suzhou, China): Xianchao Du, Xiaolin He, Yanpeng Wu, Guangwei Ren, Chuanhao Huang, Xingwu Zhu. DMPK team (Risen Pharma Tech Co., Ltd., Suzhou, China): Jinchao Ai, Yanting Ma, Chengfei Li, Yuanyuan Yan, Honggui Zhou, Qinghui Chen. Analytical chemistry team (Risen Pharma Tech Co., Ltd., Suzhou, China): Hailong Dong, Jiajun Lu.

ABBREVIATIONS

AUC, area under the concentration–time curve; BLQ, below the limit of quantification; Cpd, compounds; DCM, dichloromethane; DEA, diethylamine; DMAP, dimethylaminopyridine; EA, ethyl acetate; *F*, absolute oral bioavailability; GDP, guanosine diphosphate; GI, gastrointestinal tract; GTP, guanosine triphosphate; GTPase, guanosine triphosphatase; HBD, hydrogen-bond donor; HPLC, high-performance liquid chromatography; IP, intraperitoneal injection; LCMS, liquid chromatography-mass spectrometry; MeOH, methanol; mpk, mg per kg; NMR, nuclear magnetic resonance; N.A., not applicable; PE, petroleum ether; PK, pharmacokinetics; SGF, simulated intestinal fluid; SIF, simulated gastric fluid; SMEDDS, self-microemulsifying drug delivery systems; SNEDDS, self-nanoemulsifying drug delivery systems; TBAF, tetrabutylammonium fluoride; TEA, triethylamine; TGI, tumor growth inhibition; THF, tetrahydrofuran; UV, ultraviolet

REFERENCES

- (1) Barbacid, M. Ras genes. *Annu. Rev. Biochem.* **1987**, *56*, 779–827.
- (2) Colicelli, J. Human RAS superfamily proteins and related GTPases. *Sci. STKE* **2004**, *2004*, No. re13.
- (3) André, F.; et al. AACR project GENIE: Powering precision medicine through an international consortium. *Cancer Discovery* **2017**, *7*, 818–831.
- (4) Waters, A. M.; Der, C. J. KRAS: The critical driver and therapeutic target for pancreatic cancer. *Cold Spring Harbor Perspect. Med.* **2018**, *8*, No. a031435.
- (5) Prior, I. A.; Lewis, P. D.; Mattos, C. A. A comprehensive survey of ras mutations in cancer. *Cancer Res.* **2012**, *72*, 2457–2467.
- (6) Ostrem, J. M.; Peters, U.; Sos, M. L.; Wells, J. A.; Shokat, K. M. K-Ras(G12C) inhibitors allosterically control GTP affinity and effector interactions. *Nature* **2013**, *503*, 548–551.
- (7) Fell, J. B.; Fischer, J. P.; Baer, B. R.; Blake, J. F.; Bouhana, K.; Briere, D. M.; Brown, K. D.; Burgess, L. E.; Burns, A. C.; Burkard, M. R.; Chiang, H.; Chicarelli, M. J.; Cook, A. W.; Gaudino, J. J.; Hallin, J.; Hanson, L.; Hartley, D. P.; Hicken, E. J.; Hingorani, G. P.; Hinklin, R. J.; Meija, M. J.; Olson, P.; Otten, J. N.; Rhodes, S. P.; Rodriguez, M. E.; Savechenkov, P.; Smith, D. J.; Sudhakar, N.; Sullivan, F. X.; Tang, T. P.; Vigers, G. P.; Wollenberg, L.; Christensen, J. G.; Marx, M. A. Identification of the clinical development candidate MRTX849, a covalent KRASG12C inhibitor for the treatment of cancer. *J. Med. Chem.* **2020**, *63*, 6679–6693.
- (8) Lanman, B. A.; Allen, J. R.; Allen, J. G.; Amegadzie, A. K.; Ashton, K. S.; Booker, S. K.; Chen, J. J.; Chen, N.; Frohn, M. J.; Goodman, G.; Kopecky, D. J.; Liu, L.; Lopez, P.; Low, J. D.; Ma, V.; Minatti, A. E.; Nguyen, T. T.; Nishimura, N.; Pickrell, A. J.; Reed, A. B.; Shin, Y.; Siegmund, A. C.; Tamayo, N. A.; Tegley, C. M.; Walton, M. C.; Wang, H.-L.; Wurz, R. P.; Xue, M.; Yang, K. C.; Achanta, P.; Bartberger, M. D.; Canon, J.; Hollis, L. S.; McCarter, J. D.; Mohr, C.; Rex, K.; Saiki, A. Y.; Miguel, T. S.; Volak, L. P.; Wang, K. H.; Whittington, D. A.; Zech, S. G.; Lipford, J. R.; Cee, V. J. Discovery of a covalent inhibitor of KRASG12C (AMG 510) for the treatment of solid tumors. *J. Med. Chem.* **2020**, *63*, 52–65.
- (9) Chen, H.; Smail, J. B.; Liu, T.; Ding, K.; Lu, X. Small-molecule inhibitors directly targeting KRAS as anticancer therapeutics. *J. Med. Chem.* **2020**, *63*, 14404–14424.
- (10) Prior, I. A.; Hood, F. E.; Hartley, J. L. The frequency of ras mutations in cancer. *Cancer Res.* **2020**, *80*, 2969–2974.
- (11) Wang, X.; Allen, S.; Blake, J. F.; Bowcut, V.; Briere, D. M.; Calinisan, A.; Dahlke, J. R.; Fell, J. B.; Fischer, J. P.; Gunn, R. J.; Hallin, J.; Laguer, J.; Lawson, J. D.; Medwid, J.; Newhouse, B.; Nguyen, P.; O’Leary, J. M.; Olson, P.; Pajk, S.; Rahbaek, L.; Rodriguez, M.; Smith, C. R.; Tang, T. P.; Thomas, N. C.; Vanderpool, D.; Vigers, G. P.; Christensen, J. G.; Marx, M. A. Identification of MRTX1133, a noncovalent, potent, and selective KRAS^{G12D} inhibitor. *J. Med. Chem.* **2022**, *65*, 3123–3133.
- (12) Hallin, J.; Bowcut, V.; Calinisan, A.; Briere, D. M.; Hargis, L.; Engstrom, L. D.; Laguer, J.; Medwid, J.; Vanderpool, D.; Lifset, E.; Trinh, D.; Hoffman, N.; Wang, X.; Lawson, J. D.; Gunn, R. J.; Smith, C. R.; Thomas, N. C.; Martinson, M.; Bergstrom, A.; Sullivan, F.; Bouhana, K.; Winski, S.; He, L.; Fernandez-Banet, J.; Pavlicek, A.; Haling, J. R.; Rahbaek, L.; Marx, M. A.; Olson, P.; Christensen, J. G. Anti-tumor efficacy of a potent and selective non-covalent KRAS^{G12D} inhibitor. *Nat. Med.* **2022**, *28*, 2171–2182.
- (13) Lipinski, C. A.; Lombardo, F.; Dominy, B. W.; Feeney, P. J. Experimental and computational approaches to estimate solubility and permeability in drug discovery and development settings. *Adv. Drug Delivery Rev.* **2001**, *46*, 3–26.
- (14) Wager, T. T.; Chandrasekaran, R. Y.; Hou, X.; Troutman, M. D.; Verhoest, P. R.; Villalobos, A.; Will, Y. Defining desirable central nervous system drug space through the alignment of molecular properties, *in vitro* ADME, and safety attributes. *ACS Chem. Neurosci.* **2010**, *1*, 420–434.
- (15) Rautio, J.; Kumpulainen, H.; Heimbach, T.; Oliyai, R.; Oh, D.; Järvinen, T.; Savolainen, J. Prodrugs: Design and clinical applications. *Nat. Rev. Drug Discovery* **2008**, *7*, 255–270.
- (16) Rautio, J.; Meanwell, N. A.; Di, L.; Hageman, M. J. The expanding role of prodrugs in contemporary drug design and development. *Nat. Rev. Drug Discovery* **2018**, *17*, 559–587.
- (17) Liu, Z.; Li, W.; Wen, H. M.; Bian, H. M.; Zhang, J.; Chen, L.; Chen, L.; Yang, K. D. Synthesis, biological evaluation, and pharmacokinetic study of novel liguzinediol prodrugs. *Molecules* **2013**, *18*, 4561–4572.

- (18) Ghosh, A. K.; Brindisi, M. Organic carbamates in drug design and medicinal chemistry. *J. Med. Chem.* **2015**, *58*, 2895–2940.
- (19) Lal, R.; Sukbuntherng, J.; Tai, E. H.; Upadhyay, S.; Yao, F.; Warren, M. S.; Luo, W.; Bu, L.; Nguyen, S.; Zamora, J.; Peng, G.; Dias, T.; Bao, Y.; Ludwikow, M.; Phan, T.; Scheuerman, R. A.; Yan, H.; Gao, M.; Wu, Q. Q.; Annamalai, T.; Raillard, S. P.; Koller, K.; Gallop, M. A.; Cundy, K. C. Arbaclofen placarbil, a novel R-baclofen prodrug: Improved absorption, distribution, metabolism, and elimination properties compared with R-baclofen. *J. Pharmacol. Exp. Ther.* **2009**, *330*, 911–921.
- (20) Lal, R.; Sukbuntherng, J.; Luo, W.; Vicente, V.; Blumenthal, R.; Ho, J.; Cundy, K. C. Clinical pharmacokinetic drug interaction studies of gabapentin enacarbil, a novel transported prodrug of gabapentin, with naproxen and cimetidine. *Br. J. Clin. Pharmacol.* **2010**, *69*, 498–507.
- (21) Alouane, A.; Labruère, R.; Le Saux, T.; Schmidt, F.; Jullien, L. Self-immolative spacers: Kinetic aspects, structure–property relationships, and applications. *Angew. Chem., Int. Ed.* **2015**, *54*, 7492–7509.
- (22) Dillon, K. M.; Powell, C. R.; Matson, J. B. Self-immolative prodrugs: Effective tools for the controlled release of sulfur signaling species. *Synlett* **2019**, *30*, 525–531.
- (23) Edupuganti, V. V. S. R.; Tyndall, J. D. A.; Gamble, A. B. Self-immolative linkers in prodrugs and antibody drug conjugates in cancer treatment. *Recent Pat. Anticancer Drug Discovery* **2021**, *16*, 479–497.
- (24) Hu, L.; Quach, T.; Han, S.; Lim, S. F.; Yadav, P.; Senyschyn, D.; Trevasakis, N. L.; Simpson, J. S.; Porter, C. J. H. Glyceride-mimetic prodrugs incorporating self-immolative spacers promote lymphatic transport, avoid first-pass metabolism, and enhance oral bioavailability. *Angew. Chem., Int. Ed.* **2016**, *55*, 13700–13705.
- (25) Akinboye, E. S.; Rosen, M. D.; Denmeade, S. R.; Kwabi-Addo, B.; Bakare, O. Design, synthesis, and evaluation of PH-dependent hydrolyzable emetine analogues as treatment for prostate cancer. *J. Med. Chem.* **2012**, *55*, 7450–7459.
- (26) Maag, H. Overcoming poor permeability—the role of prodrugs for oral drug discovery. *Drug Discovery Today* **2012**, *9*, e121–e130.
- (27) Kohan, H. G.; Kaur, K.; Jamali, F. Synthesis and characterization of a new peptide prodrug of glucosamine with enhanced gut permeability. *PLoS One* **2015**, *10*, No. e0126786.
- (28) National Library of Medicine. Butyric Acid. <https://pubchem.ncbi.nlm.nih.gov/compound/264>.
- (29) National Library of Medicine. Acetaldehyde. <https://pubchem.ncbi.nlm.nih.gov/compound/177>.
- (30) Mishra, V.; Nayak, P.; Yadav, N.; Singh, M.; Tambuwala, M. M.; Aljabali, A. A. Orally administered self-emulsifying drug delivery system in disease management: Advancement and patents. *Expert Opin. Drug Delivery* **2021**, *18*, 315–332.
- (31) Koehl, N. J.; Shah, S.; Tenekam, I. D.; Khamiakova, T.; Sauwen, N.; Vingerhoets, S.; Coppenolle, H.; Holm, R. Lipid based formulations in hard gelatin and HPMC capsules: A physical compatibility study. *Pharm. Res.* **2021**, *38*, 1439–1454.
- (32) Wang, X.; Burns, A. C.; Christensen, J. G.; Ketcham, J. M.; Lawson, J. D.; Marx, M. A.; Smith, C. R.; Allen, S.; Blake, J. F.; Chicarelli, M. J.; Dahlke, J. R.; Dai, D.; Fell, J. B.; Fischer, J. P.; Mejia, M. J.; Newhouse, B.; Nguyen, P.; O’Leary, J. M.; Pajk, S.; Rodriguez, M. E.; Savechenkov, P.; Tang, T. P.; Vigers, G. P. A.; Zhao, Q. Kras^{G12D} Inhibitors. WIPO Patent WO2021041671, 2021.
- (33) Gangwar, S.; Pauletti, G. M.; Siahaan, T. J.; Stella, V. J.; Borchardt, R. T. Synthesis of a novel esterase-sensitive cyclic prodrug of a hexapeptide using an (acyloxy) alkoxy promoiety. *J. Org. Chem.* **1997**, *62*, 1356–1362.
- (34) Gallop, M. A.; Cundy, K. C.; Zhou, C. X.; Yao, F.; Xiang, J. N.; Ollman, I. R.; Qui, F. G. Prodrugs of GABA Analogs, Compositions and Uses Thereof. WIPO Patent WO2002100347, 2002.